

Springer Proceedings in Materials

Jiang Guo
Alam Md. Mahbub
Ying-Ren Chien *Editors*

Proceedings of the
9th International
Conference
on Mechanical
Manufacturing
Technology and
Material Engineering

Volume 2

 Springer

Series Editors

Arindam Ghosh, *Department of Physics, Indian Institute of Science, Bengaluru, India*

Daniel Chua, *Department of Materials Science and Engineering, National University of Singapore, Singapore, Singapore*

Flavio Leandro de Souza, *Universidade Federal do ABC, Sao Paulo, Brazil*

Oral Cenk Aktas, *Institute of Material Science, Christian-Albrechts-Universität zu Kiel, Kiel, Germany*

Yafang Han, *Beijing Institute of Aeronautical Materials, Beijing, China*

Jianghong Gong, *School of Materials Science and Engineering, Tsinghua University, Beijing, China*

Mohammad Jawaid , *Laboratory of Biocomposite Technology, INTROP, Universiti Putra Malaysia, Serdang, Malaysia*

Springer Proceedings in Materials publishes the latest research in Materials Science and Engineering presented at high standard academic conferences and scientific meetings. It provides a platform for researchers, professionals and students to present their scientific findings and stay up-to-date with the development in Materials Science and Engineering. The scope is multidisciplinary and ranges from fundamental to applied research, including, but not limited to:

- Structural Materials
- Metallic Materials
- Magnetic, Optical and Electronic Materials
- Ceramics, Glass, Composites, Natural Materials
- Biomaterials
- Nanotechnology
- Characterization and Evaluation of Materials
- Energy Materials
- Materials Processing

To submit a proposal or request further information, please contact one of the following Springer Publishing Editors according to your affiliation location:

European countries: **Mayra Castro** (mayra.castro@springer.com)

India, South Asia and Middle East: **Swati Meherishi** (swati.meherishi@springer.com)

South Korea: **Smith Chae** (smith.chae@springer.com)

Southeast Asia, Australia and New Zealand: **Ramesh Nath Premnath** (ramesh.premnath@springer.com)

The Americas: **Michael Luby** (michael.luby@springer.com)

China and all the other countries or regions, as well as topics in materials chemistry: **Maggie Guo** (maggie.guo@cn.springernature.com)

This book series is indexed in **SCOPUS** and **EI Compendex** database.

Jiang Guo · Alam Md. Mahbub · Ying-Ren Chien
Editors

Proceedings of the 9th International Conference on Mechanical Manufacturing Technology and Material Engineering

Volume 2

Editors

Jiang Guo
Dalian University of Technology
Dalian, Liaoning, China

Alam Md. Mahbub
Harbin Institute of Technology
Shenzhen, China

Ying-Ren Chien
National Ilan University
Yilan City, Taiwan

ISSN 2662-3161

ISSN 2662-317X (electronic)

Springer Proceedings in Materials

ISBN 978-981-96-5353-9

ISBN 978-981-96-5354-6 (eBook)

<https://doi.org/10.1007/978-981-96-5354-6>

© The Editor(s) (if applicable) and The Author(s), under exclusive license to Springer Nature Singapore Pte Ltd. 2025

This work is subject to copyright. All rights are solely and exclusively licensed by the Publisher, whether the whole or part of the material is concerned, specifically the rights of translation, reprinting, reuse of illustrations, recitation, broadcasting, reproduction on microfilms or in any other physical way, and transmission or information storage and retrieval, electronic adaptation, computer software, or by similar or dissimilar methodology now known or hereafter developed.

The use of general descriptive names, registered names, trademarks, service marks, etc. in this publication does not imply, even in the absence of a specific statement, that such names are exempt from the relevant protective laws and regulations and therefore free for general use.

The publisher, the authors and the editors are safe to assume that the advice and information in this book are believed to be true and accurate at the date of publication. Neither the publisher nor the authors or the editors give a warranty, expressed or implied, with respect to the material contained herein or for any errors or omissions that may have been made. The publisher remains neutral with regard to jurisdictional claims in published maps and institutional affiliations.

This Springer imprint is published by the registered company Springer Nature Singapore Pte Ltd. The registered company address is: 152 Beach Road, #21-01/04 Gateway East, Singapore 189721, Singapore

If disposing of this product, please recycle the paper.

Preface

Welcome to the proceedings of the 9th International Conference on Mechanical Manufacturing Technology and Material Engineering (MMTME 2024). This prestigious event, held in Wuhan, China, from August 2 to 4, 2024, brings together scholars, researchers, industry professionals, and other delegates from around the globe to discuss the latest advancements, challenges, and future trends in mechanical manufacturing technology and material engineering.

The theme of MMTME 2024 revolves around fostering academic exchanges, broadening research horizons, enhancing academic research and exploration, and promoting the exchange of academic achievements and industrial cooperation. This conference aims to propel the high-quality development of the mechanical manufacturing industry and the field of material engineering. It serves as a platform for sharing insights, exploring innovative ideas, and strengthening collaborations among participants.

The proceedings of MMTME 2024 encapsulates a wide array of research papers that delve into the intricacies of mechanical manufacturing technology and material engineering. It delves into the forefront of research in areas like additive manufacturing, smart manufacturing systems, and innovative material solutions, addressing the current gaps and technological challenges within the industry. The content is structured to highlight significant innovations that are poised to redefine manufacturing processes, enhance material performance, and drive sustainability in production. Key topics such as the integration of AI and IoT in manufacturing, advancements in 3D and 4D printing technologies, and the development of new sustainable materials are explored. These are critical for pushing the boundaries of what's possible in manufacturing and materials science today.

The papers in this collection have undergone a rigorous review process to ensure their quality and relevance. Each submission was evaluated by at least two to three peer reviewers for its originality, technical content, depth of research, relevance to the conference theme, contribution to the field, and readability. The acceptance of these papers reflects the high standards of academic excellence that MMTME 2024 strives to uphold.

One of the highlights of MMTME 2024 is the presence of esteemed keynote speakers and chair professors, such as Professor Hakim Naceur from the Polytechnic University Hauts-de-France and Professor Jiang Guo from Dalian University of Technology. Their speeches and presentations have enriched the conference with valuable insights and perspectives on computational mechanics, additive manufacturing, and other forefront topics. In addition to the keynote speeches, the conference also features numerous sessions dedicated to specific topics, encouraging in-depth discussions and exchanges among participants. These sessions have fostered a vibrant and collaborative atmosphere, where ideas were freely shared, and innovative solutions were explored.

This paper volume is significant as it not only encapsulates state-of-the-art research but also provides a vision for future directions in the field. It sets out to solve problems

related to efficiency, cost-effectiveness, and environmental impact in manufacturing, offering new perspectives and solutions to researchers and professionals. It is also a testament to the dedication and hard work of the authors, reviewers, and organizers.

We hope that the proceedings of MMTME 2024 will inspire further research and collaboration, leading to new breakthroughs and innovations in these critical areas. Our heartfelt thanks go to all the authors, reviewers, speakers, sponsors, and participants who made MMTME 2024 a resounding success. Look forward to welcoming you to our future conferences, continuing the tradition of academic excellence and innovation.

The Committee of MMTME 2024

Committee Member

Conference General Chair

Prof. Hakim Naceur, Polytechnic University Hauts-de-France, France
Prof. Jiang Guo, Dalian University of Technology, China

Program Committee Chair

Prof. Yongsheng Ma, Southern University of Science and Technology, China

Publication Chair

Prof. Alam Md. Mahbub, Shenzhen Graduate School of Harbin Institute of Technology, China
Prof. Ying-Ren Chien, National Ilan University, China

Organizing Committee Chair

Prof. Xinyu Li, Huazhong University of Science and Technology, China

International Technical Program Committee

Prof. Richard (Chunhui) Yang, Western Sydney University, Australia
Prof. Jinliang Luo, University of South China, China
Prof. Youwei He, University of South China, China
Prof. Yusri Yusof, Universiti Tun Hussein Onn Malaysia, Malaysia
Prof. Dr. Murat Tolga OZKAN, Gazi University, Turkey
Prof. Yudong Zhang, University of Leicester, UK
Prof. Yajun Liu, South China University of Technology, China
Prof. Prashanth Konda Gokuldoss, Tallinn University of Technology, India
Assoc. Prof. Junjun Lei, Guangdong University of Technology, China
Assoc. Prof. Xiaoyan Zhou, China University of Petroleum, China
Assoc. Prof. Xiaoming Kang, University of South China, China
Assoc. Prof. Biao Wang, Soochow University, China

Assoc. Prof. Venkata Siva Rama Prasad, St. Peters Engineering College (Autonomous),
India

Assoc. Prof. Engin Derya Gezer, Karadeniz Technical University, Turkey

Researcher Denis Andrienko, Max Planck Institute for Polymer Research, Germany

Researcher Qinghua Liu, University of Science and Technology of China, China

Assistant Researcher Yiping Gao, Huazhong University of Science and Technology,
China

Dr. Chunjiang Zhang, Huazhong University of Science and Technology, China

Dr. AHMED LEGROURI, International University of Grand-Bassam, Morocco

Dr. Hock Jin Quah, Universiti Sains Malaysia, Malaysia

Contents

Intelligent Manufacturing Process and Structure Optimization

Research on Self-Pressurization Technology of Aerospace Cryogenic Tank	3
<i>Bin Yu, Cheng Huang, Jidong Chen, Tianju Ma, and Sendong Gu</i>	
Numerical Research on Molten Pool Dynamics of Oscillating Laser Wire Additive Manufacturing	14
<i>Bowen Zheng, Junfeng Qi, Jianchao Zhang, Jingyang Li, and Zhanjiao Gao</i>	
Improving Resistive Switching Performance of Y-Doped HfO ₂ by Annealing Process	22
<i>Weisen Luo</i>	
Application of Ion Implantation Technology in the Construction of Carbon Based Spin Materials	30
<i>Hu Chen, Shen Zhou, and Weiguo Mao</i>	
Research on Balance Optimization of DF Light Car Welding Production Line	44
<i>Xiwen Wang, Hui Jin, Yanbiao Di, and Bingshuai Chen</i>	
Development of Aero Engine Materials and Manufacturing Processes	51
<i>Zijuan Liu, Xiaowei Wu, Yubing Shen, Fajia Li, and Enming Wang</i>	
Evaluation Study on the Design Scheme of Flexible Production Line for Mining Explosion-Proof Vehicles	63
<i>Yurong Liu</i>	
Performance Analysis and Optimization of Automotive B-pillar with Titanium Alloy	73
<i>Jian Zhang and Jingzhou Jiang</i>	
Research on Typical Labour-Hours Standard of Aviation Products Based on Process Feature	80
<i>Rongbo Shi, Qianqian Ye, Hongfeng Guo, and Shaoze Yuan</i>	
Optimization Design of Modular Sprocket Shaft Based on Response Surface Method	89
<i>Chunsheng Wang, Xing Sun, Dafei Tian, Yang Li, and Haoran Sun</i>	

Design of Mix Proportion and Mechanical Properties of Geopolymer Concrete 98
Wenjing Guan, Yun Xiao, Yuqing Xue, Qi Liu, and Jinyan Li

Application Analysis of Laser Cladding Technology in the Automotive Field 110
Meng Ying, Yongming Shao, and Qin Zhang

Research on Long Boring Process of Large Crawler Crane Beam Platform 116
Jianguo Liao, Honghua Bai, Xiaojian Wan, Jiabing Miao, Yong Shen, and Bing Li

Crawler Crane Surface Coating Process and Detection Analysis 123
Yang Zhang, Honghua Bai, Xiaojian Wan, Yong Shen, Jiabing Miao, and Bing Li

Research on Forging Process of TA10 Nuclear Power Valve Body 132
Shaozheng Dong, Taixu Qu, Xin Zhao, and Rui Cheng

Study on Forming Process of Large-Caliber UWB Bow-Tie Antenna with Back-Cavity 140
Runlin Li, Tao He, and Bing Wei

Development and Experimental Analysis of Electric Self-Propelled Leafy Vegetable Harvester 148
Shengjun Zhang, Xiaojun Lin, Qiang Lu, and Guoliang Meng

Research on Optimization of Sheet Metal Process for External Protective Devices of CNC Machine Tools 157
Liping Li

Optimization of Nonlinear Suspension Parameters Under Non-Gaussian Road Profile Stimulation 165
Fei Xu, Feifei Ma, Kjell Ahlin, and Jiye Tang

Effects of Ultrasonic Impact Time on Surface Morphology and Wear Resistance of Welded Joints 176
Yiming Chen, Xin Zhao, and Zhibin Yang

Dynamic Analysis and Optimization on Rotary Ear Frame of Roadheader 183
Jingxi Duan and Fuxiang Zhang

Influence of Pipe Repair Sleeve Dimension and Installation Conditions on the Girth Weld Stress 192
Mingchang Wu, Yan Xu, Di Wang, Xianying Zheng, Yongxin Lu, and Wei Qiang

Additive Manufacturing Simulation Based on Pipeline Connection Parts 200
Tongyu Zhao, Yaoyao Shi, Huaidan Liang, Junsheng Li, and Xueguang Li

Dynamic Modeling and Structure Optimization of a New Type of Gradual Hydraulic Buffer 213
Jialiang Zhou, Chenxu Yang, Tenghui Wang, Yue Liu, Xin Zhao, and Junzhou Huo

Optimization Decisions for Manufacturing/Remanufacturing Production in a Low-Carbon Environment 226
Fang Wu and Yuhang Zhou

Effect of Heat Treatment on Structure and Mechanical Properties of PAN-based Carbon Fiber 237
Junsha Wang, Xianwen Huang, Tang Yong, and Cheng Zhang

Intelligent Mechanical Design and Simulation Analysis

Design of an Independent Steer-By-Wire Corner Module Based on Double-Crank Mechanism 245
Tingting Wang, Jiawei Chen, and Xinbo Chen

Design and Modeling of a Bandpass Micro Inertial Switch 254
Wangsheng Chen, Hengbo Zhu, Zhanwen Xi, and Yun Cao

Silicon-Based MEMS Inertial Trigger Switch with a Double-Stop Mechanism for Resistance to High Overload 262
Kai Chen, Yun Cao, Hengbo Zhu, Weirong Nie, and Zhanwen Xi

Design and Implementation of Microcontroller Experimental Teaching Circuit Board 270
Zixuan Yang and Tianyu Fang

A Design of Carbon Fiber Reinforced Plastic Rear Seat Back Panel 278
Hao Xu and Jiangqi Long

Design and Simulation Analysis of the Extrusion Device of Concrete 3D Printing Device 287
Changzhong Wu, Xingyu Zhu, Liang Wu, Haibo An, Yuanyuan Lu, and Yongzhuo Wang

Design of Detection Device for Multi-Specification Precision CNC Rotary Table Performance	294
<i>Yunhui Liu, Yuyong Han, Qi Xu, Sensen Zhou, and Wei Zhang</i>	
Intelligent Agricultural Machinery Design and Implementation for Greenhouse Cultivation	303
<i>Haobin Jin, Liwei Zhou, Shuo Zhang, Zhiqiu Zhao, Fanyin Zeng, and Keshan Liang</i>	
Design and Analysis of a Cleaning Room for Assembly of Steam Generator ...	314
<i>Linhong Ji, Hangkai Shen, Wei Sheng, Jiangping Fang, Yifan Wang, and Jidan Yang</i>	
Design of Bogie Axle Box Spring Seat Fine Boring Machine and Fixture	325
<i>Taixu Qu, Shaozheng Dong, and Peng Xiao</i>	
Bogie Design of Straddle Permanent Magnet Suspension Train	332
<i>Duoli Xu and Xinyi Zhou</i>	
Structure Design and Lightweight of Box-Type Substation	346
<i>Chaofeng Yang, Chao Chen, Chao Sun, Xihao Xie, and Yezi Zeng</i>	
Design and Experiment of Crawler Self-Propelled Hydraulic Lotus Root Harvester	355
<i>Xiaojie Li, Jibin Sun, Shuangshuang Chen, and Kai Wang</i>	
Lightweight Design of Track Chassis Longitudinal Beam of Mountain Drilling Rig Based on SIMP	363
<i>Hong Zhang, Yongjian Su, Lun Wang, Yuxiang Zhu, Guowei Hu, Chaoxin Lu, Longjiang Tang, and Shanfei Zhao</i>	
Structural Design and Finite Element Simulation of Deep-Sea Pressure Resistant Electronic Cabin	376
<i>Jianbo Xu, Xiangli Kong, Chuanyang Ge, and Jiahao Xiu</i>	
Aero Engine Blade Fixture Design and Repeated Positioning Accuracy Experimental	383
<i>Shen Zhang, Bing Zhao, Dingshan Deng, and Junjie Zhao</i>	
Design and Test of Electric Driven Variable Height and Distance Film Coating Machine	392
<i>Jiao Wang, Xueqian Zuo, Yufeng Zhang, Qi Wan, Wenhao Guan, Yi Li, and Changhao Yuan</i>	

Partial Structural Design and Static Analysis of High-Altitude
Ground-Based Telescope Dome 407
Junwei Liu

Optimal Design of Traction Device of Plastic Straw Cutting Machine 417
Yunjing Tian, Yuxiang Zhang, and Rui Tian

Design and Performance Analysis of a Novel Mechanical-Hydraulic
Composite Brake 429
Zilong Zhao, Desheng Li, Tong Zhao, Keyan Ning, and Ming Han

Design and Analysis of Mixing Power of Pouring Asphalt Mixing
Equipment 438
Xiaowen Yue, Min Wang, Feng Xiong, and Fei Shang

Research on Optimization Design of Molybdenum Liner 449
*Huiming Shen, Tao Wang, Xin Liu, Xiaoning Zhang, Jintao Wang,
Guiyun Hang, and Chang Gong*

An Inkjet-Printed Nano Cellulose Electrochemical Biosensor 459
Jia Zhu and Quan Zhang

Automatic SMT Mounter for Bulk Material Recognition Based on CH32 466
Hongjun Ouyang, Yiming Liu, Jingqi Hu, Jiaqi Lu, and Xiao Wu

Signalized Analysis Model and Loop Separation Design for Tobacco
Wind Separator 474
Jinyu Chen, Weihua Ye, Qingfang Lu, Qiurong Chen, and Guiping Wu

Design and Performance Study of Prefabricated Pipe Joint Model Test 483
Yan Peng, Haiquan Gao, and Xiangxing Hu

Author Index 497

Intelligent Manufacturing Process and Structure Optimization



Research on Self-Pressurization Technology of Aerospace Cryogenic Tank

Bin Yu^{1,2(✉)}, Cheng Huang¹, Jidong Chen², Tianju Ma², and Sendong Gu²

¹ Central South University, Changsha 410083, China
cast510yb@163.com

² Lanzhou Institute of Physics, CASC, Lanzhou 730000, China

Abstract. The spacecraft propulsion system puts forward an urgent need for cryogenic propellants with high density, low pressure storage and on-orbit reusable tanks. The research on the self-pressurization mechanism of cryogenic tanks and the pressure control technology have become the main factors affecting the on-orbit application of cryogenic propellants. In this paper, a numerical model of heat transfer and pressure control of cryogenic liquid tanks under microgravity conditions is established. By comparing and analyzing the self-pressurization model of cryogenic tanks, the best finite element model is obtained, and the self-pressurization mechanism of cryogenic tanks is analyzed, which lays a foundation for low temperature pressure control. The research content of the follow-up work on the pressure control of cryogenic propellant on-orbit storage is proposed, which provides reliable theoretical support for the storage and transportation of cryogenic propellant in space in the future.

Keywords: Cryogenic propellant · propellant tank · Self-pressurization · Liquid mixing · Active cooling

1 Introduction

Low-temperature propellants such as liquid xenon and liquid krypton are used in satellite electric propulsion engines, and low-temperature propellants such as liquid hydrogen and liquid oxygen are used in satellite chemical propulsion engines [1–3]. Low-temperature propellants are recognized as the most economical and efficient chemical propellants for future space and space orbit transfer, and are the preferred propellants for future space spacecraft. However, in the process of space flight, due to the influence of space heat load such as solar radiation, earth infrared radiation, planetary albedo, and cold black background, the low-boiling cryogenic propellant is heated and evaporated, thereby increasing the internal pressure of the cryogenic tank, resulting in overpressure damage of the cryogenic tank. Although the pressure control strategy of gaseous cryogenic propellant emptying can effectively solve the overpressure problem, it causes the waste of propellant and the reduction of total specific impulse. In addition, the exhaust will also interfere with the flight attitude. It can be seen that the design of long-term on-orbit cryogenic storage system is one of the key technical problems in space flight.

The key problem of cryogenic liquid space storage is the pressure control technology of the tank under microgravity conditions [4–6]. During the filling of cryogenic liquid propellant and the operation of the aircraft, the pressure of the cryogenic tank increases due to the external heat load, resulting in the evaporation of some cryogenic liquid, which makes the cryogenic liquid in the tank in a two-phase state and forms a pillow area inside the tank. Usually, due to the existence of gravity, there is an obvious gas-liquid interface in the tank. However, under microgravity, the shape and position of the ullage are uncertain, which affects the efficient implementation of active cooling measures and increases the difficulty of venting, which has a great impact on the long-term on-orbit storage of cryogenic propellants [7–9].

By adding a propellant management device, the accurate positioning of the fluid distribution of the cryogenic propellant can be realized. The cryogenic propellant fluid mixing technology is used to make the propellant form a circulating fluid inside the tank. The cryogenic fluid after the refrigerator is cooled is re-sprayed into the tank to cool the inside of the tank, thereby achieving pressure control [10–12]. Therefore, it is of great academic value and engineering application significance to obtain the basic theoretical research on the heat and mass transfer and thermal stratification mechanism of cryogenic liquid two-phase flow under microgravity conditions, and to propose the best strategy of pressure control, which has become one of the key technologies of space on-orbit propellant pressure control technology.

The aerospace cryogenic tank can achieve ZBO or RBO technical indexes by using active cooling static heat conduction coupling technology, active cooling liquid mixing heat coupling technology and cooling screen technology. It is necessary to select the appropriate technical scheme according to different working conditions of the cryogenic tank. According to the functional requirements of spacecraft chemical propulsion and electric propulsion system, combined with the functional requirements of storage, anti-sloshing and supply of space propellant tank surface tension management device, as well as the requirements of tank structure and propellant physical properties, the combination of active cooling and liquid mixing technology is more in line with the requirements of technological development. Based on the analysis of the technical characteristics and difficulties of thermal stratification of aerospace cryogenic tanks, for cryogenic tanks or spherical cryogenic tanks, the active cooling liquid mixing thermal coupling technology adopts the central shaft jet rod radial liquid mixing technology scheme, which has the advantages of high efficiency, low power consumption, simple structure and light weight.

2 Comparative Analysis of Calculation Models

2.1 Technology Analysis

Under space microgravity, the propellant inside the tank exists in the form of gas-liquid two-phase flow. Due to the influence of micro-acceleration, non-uniform heat source, thermal transient and other factors, the thermal stratification inside the tank is caused. The first is the non-uniformity of temperature. The saturated vapor pressure is different in different temperature ranges of cryogenic liquid working medium. Excessive temperature leads to abnormal increase of pressure. The uncertainty of gas-liquid position inside the tank leads to the internal gas-liquid two-phase flow state and internal thermal

stratification. The increase of internal pressure causes gas-liquid mixing and propellant loss, which leads to the decrease of propellant capacity and satellite life.

The key to satellite pressure control is to control the pressure of the superheated gas phase. At present, liquid mixing and stirring are mainly used at home and abroad, and the superheated gas phase is stirred by supercooled liquid phase cooling, so as to eliminate thermal stratification, effectively control the internal pressure of the tank, and eliminate the problem of gas-liquid mixing of propellant.

During the stable operation of the cryogenic tank in the whole life cycle, it will be affected by the environmental heat load, and the pressure in the tank will rise accordingly, accompanied by thermal stratification. Thermal stratification refers to the temperature gradient distribution of the fluid working medium within a certain range, which is a typical problem of uneven energy distribution. In order to ensure the safety of the storage system, the research of this problem has become a key technical problem to be solved urgently. Therefore, in the design stage of cryogenic tank, it is necessary to focus on the thermodynamic change process of internal pressure rise caused by heat leakage of wall and support.

2.2 Geometric Model

The cryogenic storage tank in Fig. 1, the tank includes the upper head of the inner tank, the inner tank cylinder, the lower head of the inner tank, the inlet, the jet rod and the outlet. Among them, the axial and circumferential directions of the jet rod are uniformly distributed with nozzles.

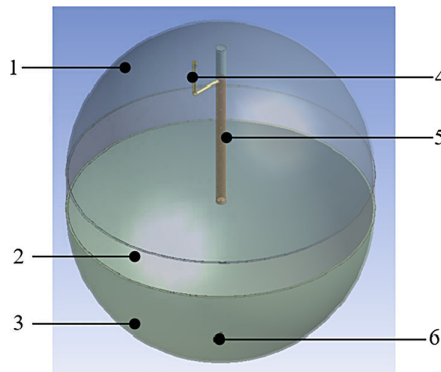


Fig. 1. Three-dimensional model of cryogenic storage tank

2.3 Comparative Study of Models

During the stable operation of the cryogenic tank in the whole life cycle, it will be affected by the environmental heat load, and the pressure in the tank will rise accordingly, accompanied by thermal stratification. Thermal stratification refers to the temperature

gradient distribution of the fluid working medium within a certain range, which is a typical problem of uneven energy distribution. In order to ensure the safety of the storage system, the research of this problem has become a key technical problem to be solved urgently. Therefore, in the design stage of cryogenic tank, it is necessary to focus on the thermodynamic change process of internal pressure rise caused by heat leakage of wall and support.

The self-pressurization phenomenon in the cryogenic tank is mainly caused by the following two factors: First, the gas mass fraction and dryness increase due to the evaporation process and wall heat leakage. However, the volume ratio of the gas phase zone in the cryogenic tank is limited, which is equivalent to inflating into a finite volume container, so the pressure and temperature of the gas will increase successively. Second, because the liquid phase density will gradually decrease with the increase of liquid temperature, the volume expansion of the liquid phase produces a certain amount of compression work in the gas phase region, which is manifested in the form of increased gas phase pressure. Therefore, in order to improve the prediction ability of numerical simulation of self-pressurization process, the selection of accurate gas model and liquid phase density model is an important means to achieve this goal.

Using the material model of nitrogen working medium in Fluent software, the initial temperature of liquid phase is set to be 73 K, the initial temperature of gas phase is 78 K, the boundary condition of liquid phase is a constant temperature boundary of 100 K, the boundary of gas phase is adiabatic boundary, and the initial filling rate is 50%. The three simulation technology routes are shown in Table 1. The simulation results are shown in Figs. 2, 3 and 4.

Table 1. The three simulation technology routes.

Simulation	Scheme 1	Scheme 2	Scheme 3
Gas phase	Ideal gas-state equation	P-R state equation	R-K-S equation
Liquid phase	Fixed value	Boussinesq	Boussinesq

The gas-liquid phase change process of three groups of low-temperature working fluids in the simulation is analyzed. It is found that when the liquid phase density is treated in a fixed value, the proportion of liquid phase volume decreases gradually with the evaporation process, and the proportion of gas phase volume increases significantly. For the gas-liquid phase change process obtained by the Boussinesq approximation method, the liquid phase expands with the increase of temperature, and the gas phase mass fraction increases, but the volume fraction does not increase, but it is slowly reduced by the expansion liquid phase compression. The three sets of simulations correspond to different combinations of gas and liquid phase density models. According to the gas phase temperature and density values obtained by simulation, the corresponding theoretical pressure values are calculated. Compared with the simulated pressure values, the gas phase density is obtained by using the R-K-S real gas equation and the liquid phase density. The simulation value obtained by the combination of the Boussinesq approximation model is closer to the theoretical value.

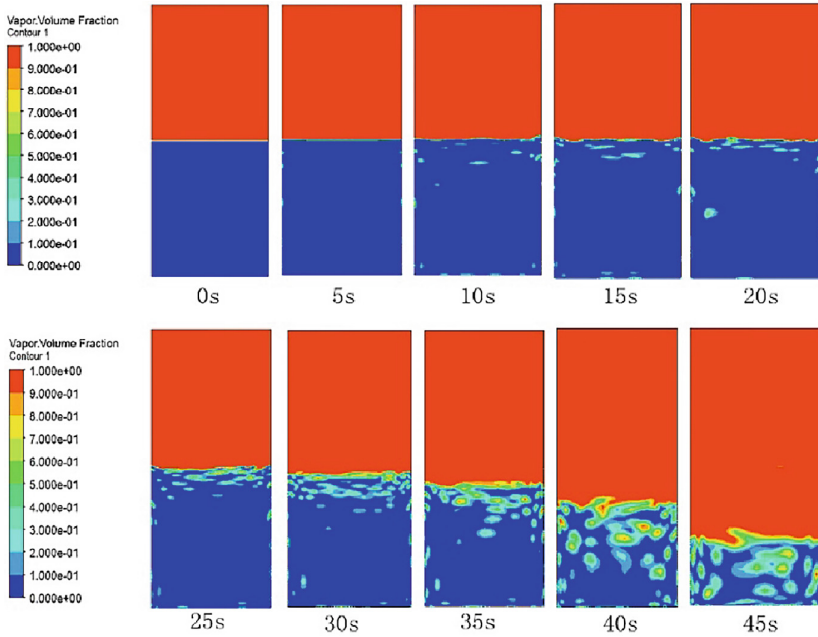


Fig. 2. Combined simulation results of ideal gas model and liquid phase constant density

3 Simulation Analysis of Pressurization

3.1 Finite Element Model

The finite element mesh is generated by the finite element software. The regular tetrahedral mesh is used in the column section, and the mesh of the upper and lower ellipsoid head area is segmented. The mesh refinement is carried out for the near wall surface, and 10 layers of boundary layer are set up. The number of grids is 5528, and the finite element model is shown in Fig. 5.

3.2 Solution of Self-Pressurization Numerical Model of Cryogenic Tank

The most fundamental reason for the formation of the self-pressurization phenomenon is the evaporation of the liquid phase and the volume expansion of the gas-liquid two-phase after heating caused by the heat leakage of the low-temperature tank wall and the support. The self-pressurization process of the liquid tank is simulated, and the pressure and temperature in the tank are obtained with time. The change process reveals the heat and mass transfer process between the gas and liquid phases in the liquid cryogenic tank. Different boundary conditions and environmental conditions are set to study the self-pressurization law of liquid cryogenic tank, which mainly involves the law of different wall heat flux, different liquid filling rate and different gravity environment. The simulation results of low temperature pressurization are shown in Figs. 6, 7 and 8, respectively.

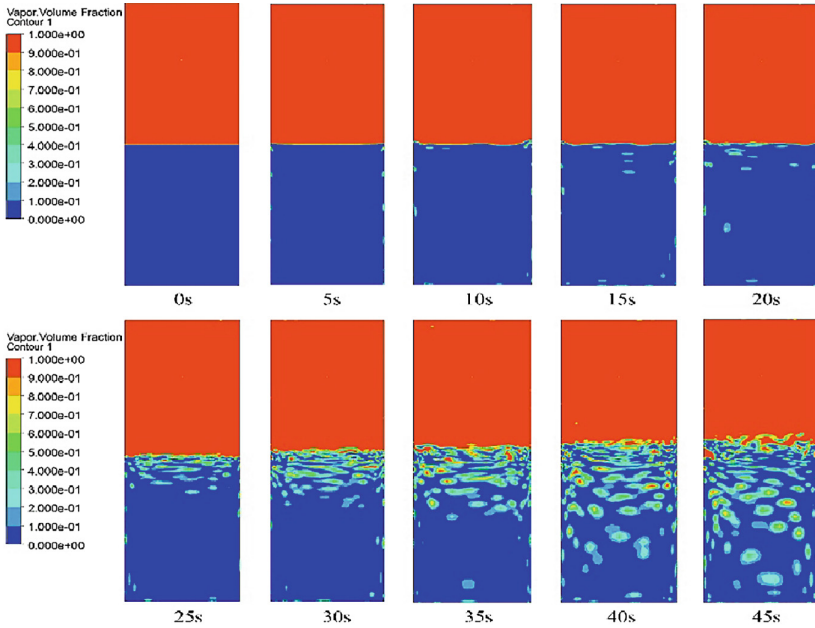


Fig. 3. Combined simulation results of P-R gas model and Boussinesq approximation of liquid phase density

Under normal gravity, using the axisymmetric two-dimensional tank model, the transient simulation analysis process of the gas phase pressure from 82 kPa to 118.8 kPa experienced a total of about 1330s, and the distribution of temperature, pressure and velocity in the tank at the end time was obtained. Due to the effect of gravity, there are different degrees of hydrostatic pressure in the liquid phase along the axial direction. Therefore, there is an obvious pressure gradient in the liquid phase in the pressure cloud diagram, the gas phase is evenly distributed, and the pressure is consistent. In the ground parking stage, due to the action of hydrostatic pressure, the maximum pressure position in the tank is at the bottom of the tank, and the maximum pressure corresponding to 1330 s is 126.2 kPa. From the temperature cloud map, it can be seen that there are temperature stratification and uneven distribution in the gas-liquid region, and the fluid temperature near the wall is high. Because the heat and mass exchange in the box mainly exists in the gas-liquid interface layer, the velocity streamline distribution at the interface layer can be observed through the velocity cloud map distribution, which reveals the mass and energy exchange process in the gas-liquid region at the interface layer to a certain extent.

From the gas phase temperature and pressure change curves, it can be seen that the drop section caused by the temperature gradient setting in the initial stage. By comparing the liquid phase temperature change curve and the gas phase temperature change curve, the gas phase temperature has a sharp change in a short period of time, and after reaching the thermodynamic equilibrium in the tank, it begins to show a steady upward trend. Due to the violent movement of gas micro-clusters in the gas phase region, the gas phase

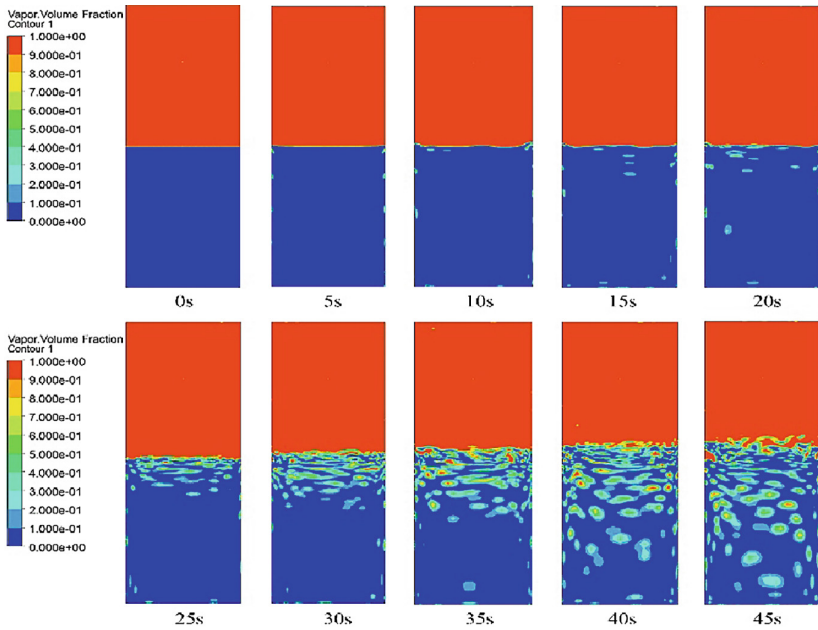


Fig. 4. Combined simulation results of R-K-S gas model and Boussinesq approximation of liquid phase density

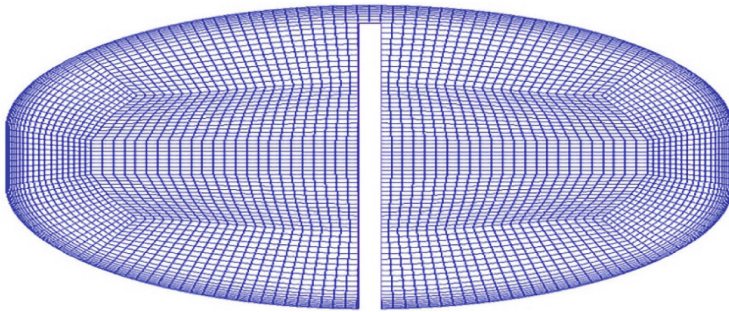


Fig. 5. Finite element model of cryogenic tank

heating curve fluctuates, while the liquid phase heating curve is stable. Compared with the liquid phase heating curve, the gas-liquid phase heating curve shows an approximately uniform heating rate. This phenomenon explains the initial condition setting that the gas-liquid phase wall heat flux density value corresponding to the initial liquid phase filling rate of 50% is close to the same.

In addition, 10 temperature monitoring points were set up in the vertical direction near the central axis, and the corresponding temperature curve changes at different times along the axial direction were obtained. It can be clearly observed that there are different degrees of temperature gradient distribution in the gas-liquid region at different times,

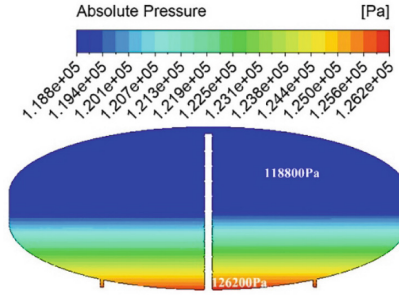


Fig. 6. Simulation results of pressure distribution in 1330 s cryogenic tank

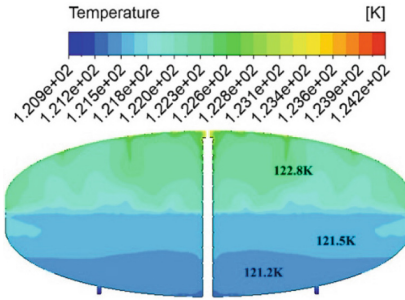


Fig. 7. Simulation results of temperature distribution in 1330 s cryogenic tank

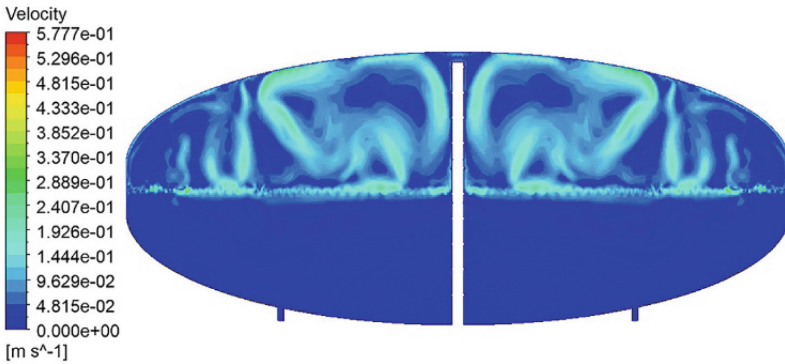


Fig. 8. Simulation results of velocity distribution in 1330 s cryogenic tank

that is, thermal stratification. Compared with the liquid phase temperature change at the same axial position at the same time interval, the displacement of the temperature point to the right is almost equal. Combined with the approximate linear liquid phase heating curve, the thermodynamic process of the liquid phase temperature change under the uniform wall heat flux boundary is well explained. The greater the range of parameters in the cryogenic tank. From the perspective of convective heat transfer formula, when the

heat flux increases and the heat transfer coefficient remains constant, the corresponding change temperature value is larger, that is, the temperature in the liquid krypton cryogenic tank becomes larger.

The evaporation and condensation process of cryogenic propellant is mainly carried out through the gas-liquid interface layer. In the normal gravity environment, the gas-liquid phase has a clear interface, and the gas-phase heating by natural convection is relatively stable and efficient, so the gas-phase pressure curve shows a regular and stable upward trend. With the decrease of gravity, the gas-liquid phase in the liquid krypton cryogenic tank gradually tends to disperse, and the gas-liquid phase interface is continuously reconstructed with time. At this time, the heat exchange efficiency is low and the heating is uneven, so the self-pressurization rate slows down.

3.3 Self-Pressurization Test and Liquid Mixing Test

The test mainly includes two parts: pressurization and depressurization. The pressurization mainly relies on the heat leakage of the tank to achieve self-pressurization. The depressurization realizes the cooling of the propellant by opening the cryogenic pump and the refrigerator. The radial jet liquid mixing is used to eliminate the thermal stratification and reduce the tank temperature. The test results are shown in Fig. 9, and the test results of the pressurization interval are approximately consistent with the simulation analysis results.

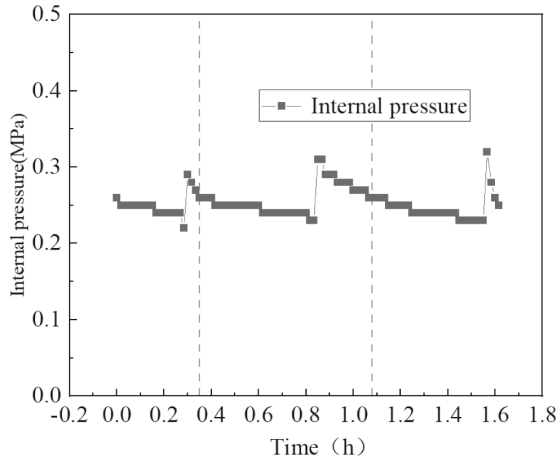


Fig. 9. Self-pressurization and liquid mixing test

3.4 Parameter Sensitivity Analysis of Self-Pressurization and Depressurization

The wall heat leakage is the main factor for the self-pressurization phenomenon in the liquid krypton cryogenic tank. First, in the closed tank, the higher the heat flux, the higher

the pressurization rate. However, because the gas phase pressurization rate is greater than the heating rate of the saturated phase transition temperature, the temperature at the gas-liquid interface is lower than the phase transition saturation temperature. According to the phase transition formula of the evaporation and condensation process, the process delays the liquid phase evaporation to a certain extent. Second, because the liquid phase is heated by the wall heat flow, the liquid phase temperature rises, and then the liquid phase volume expands. This process has a certain compensation for the downward trend of the liquid level in the box.

The temperature of the refrigerator heat exchanger and the pumping speed of the cryogenic pump are the main factors affecting the depressurization of the tank. The lower the temperature of the refrigerator, the greater the cooling capacity of the tank, the higher the pumping speed of the cryogenic pump, the higher the liquid injection speed, and the greater the cooling capacity of the tank.

4 Conclusion

The ideal gas model and the fixed liquid phase density model are often used for the gas-liquid phase density model, so there is a certain gap between the simulation results and the actual thermal physical process. Based on this, this chapter first uses liquid nitrogen cryogenic working fluid to simulate and compare the gas-liquid density model combination of cryogenic working fluid, that is, the gas phase temperature and density values obtained by simulation, the corresponding theoretical pressure values are calculated, and the simulation pressure values are compared. Finally, it is found that the simulation value obtained by the combination of the gas phase density using the R-K-S actual gas equation and the liquid phase density using the Boussinesq approximation model is closer to the theoretical value.

Since there is no gas-liquid two-phase material model for a specific working medium in the finite element software material library, a two-phase material model for analyzing the working medium is built, and the above-mentioned gas-liquid two-phase density model combination is used for numerical calculation and verification. The results show that the simulation value of the gas phase pressure obtained by the self-built working medium is highly consistent with the theoretical value curve. Compared with the curve obtained by the liquid nitrogen working medium, the curve change trend is basically the same, which proves the correctness of the established two-phase material model of the working medium. At the same time, it is proved that the selected gas-liquid two-phase density model of cryogenic working fluid has better calculation and prediction performance for working fluid, which is closer to the theoretical value and improves the scientificity of subsequent simulation research.

References

1. Yu, B., Huang, C., Yang, W.B.: Development technique of large scale composite tank for space vehicle. *Press. Vessel Technol.* **43**(2), 1–9 (2022)
2. Yu, B., Zhang, J.J., Gu, S.D., et al.: Structure design study of composite overwrapped pressure vessel with plastically working liner. *J. Propulsion Technol.* **43**(2), 1–9 (2022)

3. Huang, C., Liu, D.B., Wu, H.Q., et al.: Application prospects of composite propellant tanks in domestic launch vehicles. *J. Shenyang Aerosp. Univ.* **33**(2), 27–35 (2016)
4. Liu, Z., Li, Y., Gao, P.: Heat transfer analysis of cryogenic tank covered with vapor-cooled shield. *J. Eng. Thermophys.* **40**(3), 629–634 (2019)
5. Yu, J., Zhang, Q., Kang, H., et al.: Comprehensive optimization design of VCS composite thermal insulation structure for cryogenic propellant tank. *Vacuum Cryogenics* **27**(2), 165–170 (2021)
6. Tuo, Z.: The heat transfer study of cryogenic vapor cooled shield compounded insulation, pp. 1–58. Lanzhou University of Technology, Lanzhou (2016)
7. Guan, C.-B., Shen, Y., Wei, Y.-M., et al.: Review and prospect of xenon feeding system for space electric thruster. *J. Astronaut.* **41**(3), 251–260 (2020)
8. Wang Xi, Wang Jue, Rong Yi, et al.: Research on cryogenic axial-jet mixing in thermodynamic vent system. *Missiles Space Veh.* (4), 46–50 (2018)
9. Li, P., Sun, P., Sheng, M., et al.: Investigation on passive boil-off control scheme for orbital storage of cryogenic propellant in orbital transfer spacecraft. *Manned Spaceflight* **24**(1), 91–97 (2018)
10. LI, Y.-J., Gao, X., Chen, H., et al.: Similarity analysis of different replacement gases for cryogenic propellant loading system. *J. Propulsion Technol.* **39**(3), 703–708 (2018)
11. Zheng, Y.: Study on the flow and heat transfer characteristics of cryogenic propellant filling process under special conditions, 1–127. Zhejiang University, Zhejiang (2020)
12. Shi, Q., Tu, C., Liu, Y., et al.: Research progress on standard devices for cryogenic fluid flow. *Cryogenic/Cooling* **51**(11), 51–59 (2023)



Numerical Research on Molten Pool Dynamics of Oscillating Laser Wire Additive Manufacturing

Bowen Zheng, Junfeng Qi^(✉), Jianchao Zhang, Jingyang Li, and Zhanjiao Gao

Beijing Satellite Manufacturing Co. LTD., Beijing 100190, China
qjfcn@163.com

Abstract. Compared to arc additive manufacturing, Oscillating Laser Wire Additive Manufacturing (O-LWAM) technology provides lower raw material costs, higher material utilization, and faster deposition. However, rapid melting, solidification, and cooling can cause defects like warping, cracks, pores, poor fusion, and coarse columnar grains. By employing different laser beam oscillation methods, O-LWAM enhances energy distribution and molten metal flow to reduce defects and improve material performance. This paper establishes numerical models to visualize and analyze the effects of oscillating lasers on energy distribution and molten pool evolution, offering a reference for process parameter optimization for performance enhancement in additive manufacturing.

Keywords: Numerical Models · Additive Manufacturing · Molten Pool Dynamics · Energy Distribution

1 Introduction

Wire Laser Additive Manufacturing (WLAM) technology uses a laser as a heat source and controls the laser head and wire feeding device to move dynamically in space relative to the deposition layer through a KUKA robot to create additive products. Compared to arc additive manufacturing, the advantages of using a laser beam as a heat source in WLAM technology include high forming accuracy, low thermal deformation of products, and ease of automation and intelligence. Utilizing wire material provides benefits such as low raw material cost, high material utilization rate, and fast deposition speed. However, in the additive process, metal melting, solidification, and cooling are completed in a very short time, causing severe temperature fluctuations, which can easily lead to defects such as warping, cracks, pores, poor fusion, and coarse columnar grains.

Aluminum alloys, as lightweight metal materials widely used in the aerospace field, tend to form defects during printing due to their active chemical properties, high laser reflectivity, and easy combination with oxygen, which reduces product quality [4]. By combining different laser beam oscillation methods, the oscillating wire laser additive manufacturing (O-WLAM) technology can enhance the flow of the molten metal and improve the energy field distribution, thereby suppressing defects and improving material

performance. Dai et al. [3] conducted a detailed comparison of the melting of TC4 in additive manufacturing using various laser oscillation methods and characterized the microstructure of TC4 under different oscillation parameter.

Studying the microstructure and mechanical properties of oscillating laser wire additive manufacturing of titanium alloys and aluminum alloys can guide structural design and feedback production, which has significant engineering value. Despite numerous studies on oscillating laser wire additive manufacturing, there remain gaps in understanding the relationship between energy distribution, molten metal flow behavior, defect suppression mechanisms in the additive process of light metals such as titanium and aluminium [1, 7].

This paper establishes a numerical model of the laser heat source and a high-fidelity heat flow coupling model. From the perspectives of oscillating laser heat source intensity and the resulting metal flow, it visualizes both models to respectively explain the roles of oscillating laser in defect and coarse columnar grains suppression of metal materials in additive manufacturing, providing a reference for the optimization of actual process parameters and the enhancement of additive product performance.

2 Numerical Simulation Modeling

2.1 Energy Flux Model

To better match the actual conditions of oscillating laser wire additive manufacturing, the heat source in this oscillating laser heat source model uses a planar Gaussian heat source. The heat source equation is as follows [2]:

$$q(x, y, t) = \frac{3\eta P}{\pi r_0^2} \exp\left(-3 \frac{(x - x(t))^2 + (y - y(t))^2}{r_0^2}\right) \quad (1)$$

where η is the material's absorptivity to the laser, r_0 is the laser beam radius used to measure laser quality, and $x(t)$, $y(t)$ are used to describe the oscillating laser trajectory. The parametric equation for a circular oscillating laser is as follows [4]:

$$\begin{cases} y(t) = y_0 - A \sin(2\pi ft) \\ x(t) = x_0 + vt + A \sin(2\pi ft + \frac{\pi}{2}) \end{cases} \quad (2)$$

A is the amplitude of the laser oscillation, f is the frequency of the laser oscillation, and v is the speed at which the heat source moves.

The energy distribution formula of the laser acting on the surface of the metal material is as follows [5]:

$$E(x, y) = \int_0^1 q(x, y, t) dt \quad (3)$$

Integrating Eq. (1) over the interval $t \in [0, 1]$ [0, 1] to obtain the energy distribution intensity of the laser heat source acting on the metal surface at various positions within a cycle.

2.2 High Fidelity Model

Considering the liquid metal in the molten pool as a Newtonian incompressible fluid, its continuity equation is [6]:

$$\nabla \cdot (\vec{v}) = 0 \quad (4)$$

For the momentum conservation, the governing equation can be expressed to identify the driving forces [6]:

$$\begin{aligned} \frac{\partial(\rho\vec{v})}{\partial t} + \nabla \cdot (\rho\vec{v} \otimes \vec{v}) = & -\nabla P + \nabla \cdot (\mu\nabla\vec{v}) + \rho\vec{g} \\ & + \rho g \beta(T - T_L) - \frac{K_0(1 - f_l)^2}{f_l^3 + B} \vec{v} + S_m \end{aligned} \quad (5)$$

In this context, ρ represents the density of the material, t denotes time, P stands for pressure, and μ is the dynamic viscosity of the fluid. B is introduced as a negligible value to prevent mathematical singularities. The buoyancy effect is modeled using the Boussinesq approximation, while the Darcy term approximates the resistive damping in the mushy zone, where K_0 represents the resistance coefficient and f_l indicates the fraction of the liquid phase. S_m encompasses the resultant body force from various surface effects, including surface tension, the Marangoni effect, the pressure due to evaporation, and laser pressure [8].

Evaporative recoil pressure arises when metal vapor molecules collide with the liquid surface. The Clausius-Clapeyron equation allows us to estimate this as 0.54 times the equilibrium vapor pressure at the liquid interface, as discussed by Ke et al. [8]

$$\vec{F}_{\text{recoil}} = 0.54\vec{F}_0 \exp\left(\frac{\Delta H_V^*(T - T_V)}{RTT_V}\right) \cdot \vec{n} \quad (6)$$

Surface tension and Marangoni force act on the surface of the molten metal fluid. Due to the large temperature gradient on the surface of the molten pool, the metal fluid is usually driven to flow tangentially along the surface. The form is as follows [8]:

$$f = \sigma\vec{n}\kappa + \frac{d\sigma}{dT}[\nabla T - \vec{n}(\vec{n} \cdot \nabla T)] \quad (7)$$

where σ is the surface tension coefficient of the liquid metal, $\frac{d\sigma}{dT}$ is the surface tension temperature coefficient, \vec{n} and κ represent the normal vector and curvature of the free surface of the molten pool, respectively [9].

The energy equation is [8]:

$$\frac{\partial\rho H}{\partial t} + \nabla \cdot (\rho\vec{v}H) = \nabla \cdot (k\nabla T) + S_h \quad (8)$$

where H represents enthalpy, k is the thermal conductivity of the material, and S_h is the volumetric heat source and heat loss which is same to the 2.1.

3 Results and Discussion

3.1 Energy Distribution

Figure 1 illustrates the variation in energy distribution of the laser, set at 3000 W with an oscillation frequency of 100 Hz, under varying amplitudes. In the depicted scenarios, the absence of oscillation leads to a sharp decline in energy density as distance from the centerline increases. Conversely, upon introducing oscillations, there's a marked shift in energy distribution patterns across Fig. 1 (b), (c), and (d). Notably, the 'double peak' pattern emerges as a distinct feature, contrasting sharply with the 'single peak' scenario by exhibiting a lesser drop between peaks and a more evenly spread energy distribution. The figure captures energy densities at various amplitudes ($A = 0, 0.5, 1, \text{ and } 1.5$), documenting maximum values at 319.1, 193.4, 128.8, and 103.5 J/mm^2 , respectively. These values demonstrate a pronounced decrease in energy density concurrent with increased laser oscillation amplitudes.

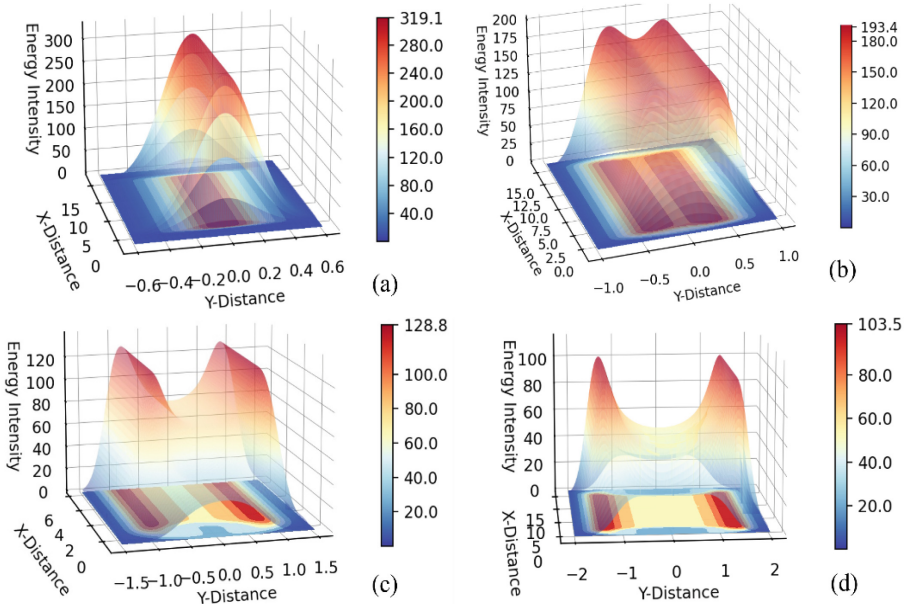


Fig. 1. The energy distribution (J/mm^2) on additive varying with oscillating amplitudes (a) $A = 0$, (b) $A = 0.5$ mm, (c) $A = 1$ mm (d) $A = 1.5$ mm.

Figure 1 illustrates that with increasing oscillation amplitudes, the maximum energy density on the surface experiences a notable reduction and the distribution of energy becomes more evenly spread. This contrasts sharply with the effects observed using a static linear laser heat source, where increased amplitude leads to a lower temperature gradient. The combined effects of the temperature gradient G and the solidification rate R crucially influence the morphology and dimensions of grains formed during